

Transcriptome-based *in silico* screening in human motor neurons with ALS-associated mutations in *TARDBP/TDP-43*



Sarah Lépine^{1,2}, Gilles Maussion¹, Alexandria Schneider¹, Angela Nauleau-Javaudin^{1,3}, Georgina Jiménez Ambriz⁴, Dan Spiegelman⁴, María José Castellanos-Montiel¹, Narges Abdian¹, Anna K. Franco-Flores¹, Ghazal Haghi¹, Lale Gursu¹, Mathilde Chaineau^{1,*}, and Thomas M. Durcan^{1,*}

¹Early Drug Discovery Unit (EDDU), The Neuro-Montreal Neurological Hospital and Institute, Department of Neurology and Neurosurgery, McGill University, Montreal, QC

²Faculty of Medicine and Health Sciences, McGill University, Montreal, QC

³Faculty of Medicine, Université de Montréal, Montreal, QC

⁴The Neuro Bioinformatics Core Facility, The Neuro-Montreal Neurological Institute and Hospital, McGill University, Montreal, QC

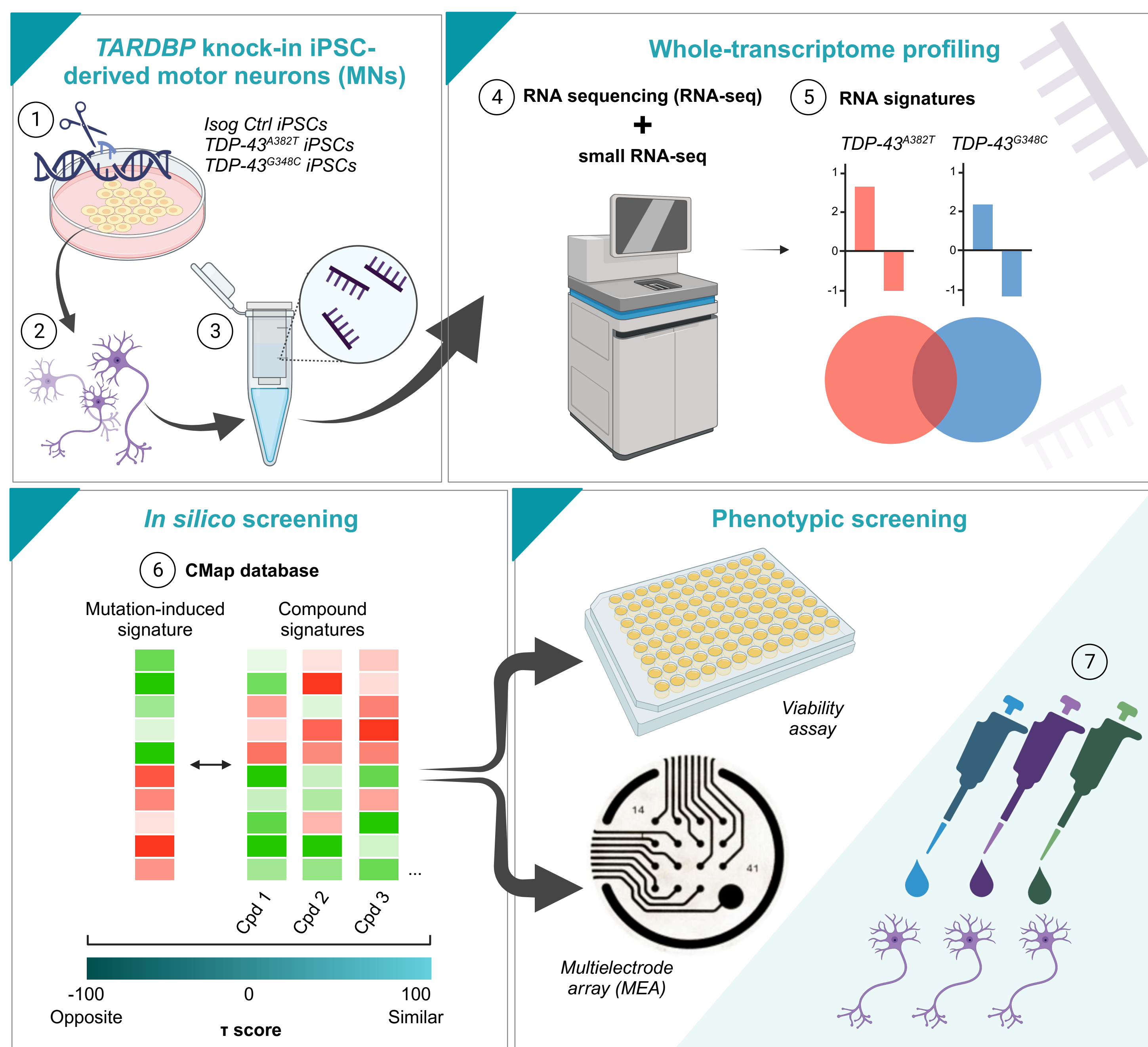
INTRODUCTION

Accumulating evidence implicates perturbed RNA homeostasis in ALS. A pathological hallmark of this disease is the nuclear depletion and cytoplasmic aggregation of the RNA-binding protein TDP-43, involved in nearly all aspects of RNA processing [1]. Furthermore, a subset of ALS patients carries mutations in *TARDBP* (coding for TDP-43). Yet, how disease-associated mutations in *TARDBP* affect RNA processing remains poorly understood. Determining the transcriptome alterations that arise in presence of mutations may inform the development of transcriptome-correcting therapies able to normalize several disease pathways simultaneously. This drug discovery paradigm known as “transcriptome reversal” was previously applied to neurological diseases including epilepsy [2], schizophrenia [3], and frontotemporal dementia [4], and yet remains largely unexplored in the ALS field.

OBJECTIVES

We aimed to identify transcriptomic alterations induced by *TARDBP* mutations and investigate potential transcriptome-correcting therapeutic strategies in human motor neurons (MNs) derived from induced pluripotent stem cells (iPSCs).

METHODS



RESULTS

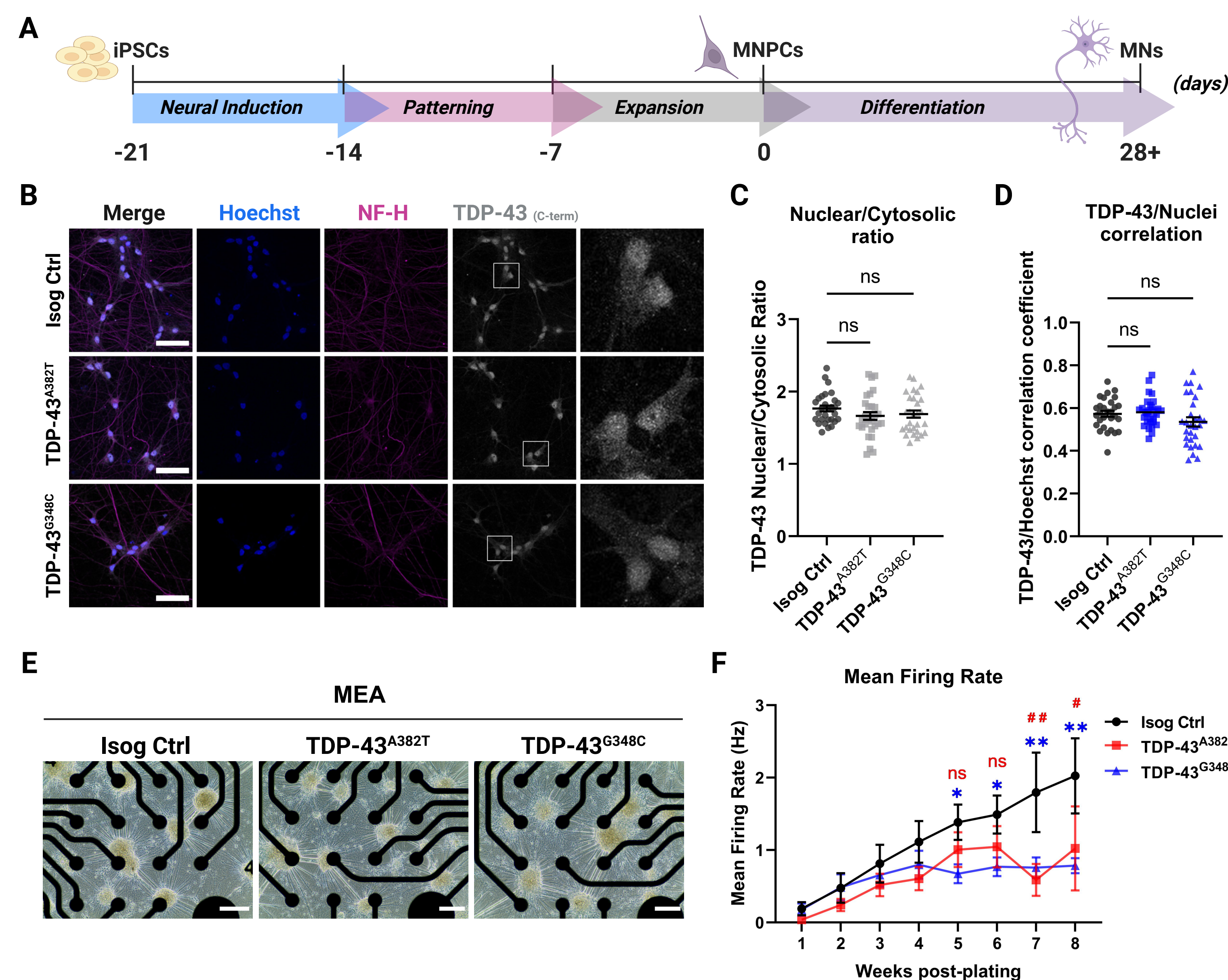


Figure 1. Mutant MNs are dysfunctional in absence of TDP-43 pathology. (A) Differentiation of MNs from iPSCs. (B-D) Representative immunostaining (B) and quantification (C,D) of TDP-43 subcellular localization in MNs differentiated for 6 weeks. Scale bar, 50 μ m. n=5. (E) Phase-contrast images of MNs differentiated on 24-well multielectrode (MEA) plates. Scale bar, 250 μ m. (F) Longitudinal changes in mean firing rate of MNs. n=11. All data shown as mean \pm SEM. * p <0.05, ** p <0.01.

RESULTS

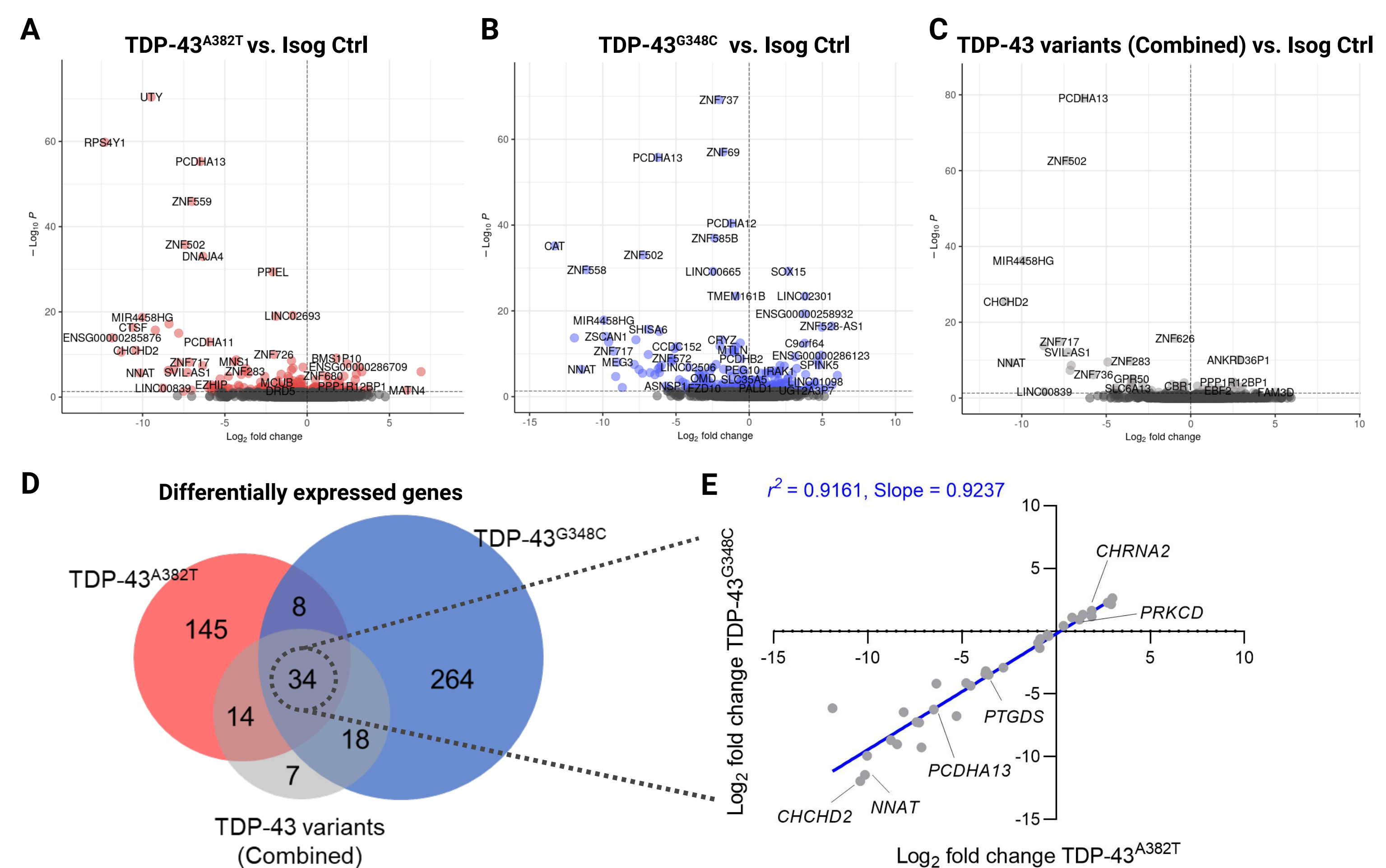


Figure 2. Identification of a shared gene expression signature in TDP-43^{A382T} and TDP-43^{G348C} MNs by RNA-seq. (A-D) Volcano plots (A-C) and Venn diagram (D) comparing differentially expressed genes (DEGs) in TDP-43 MNs relative to isogenic control (false discovery rate of 5%). (E) Scatter plot showing a strong correlation between fold changes of overlapping DEGs. n=5.

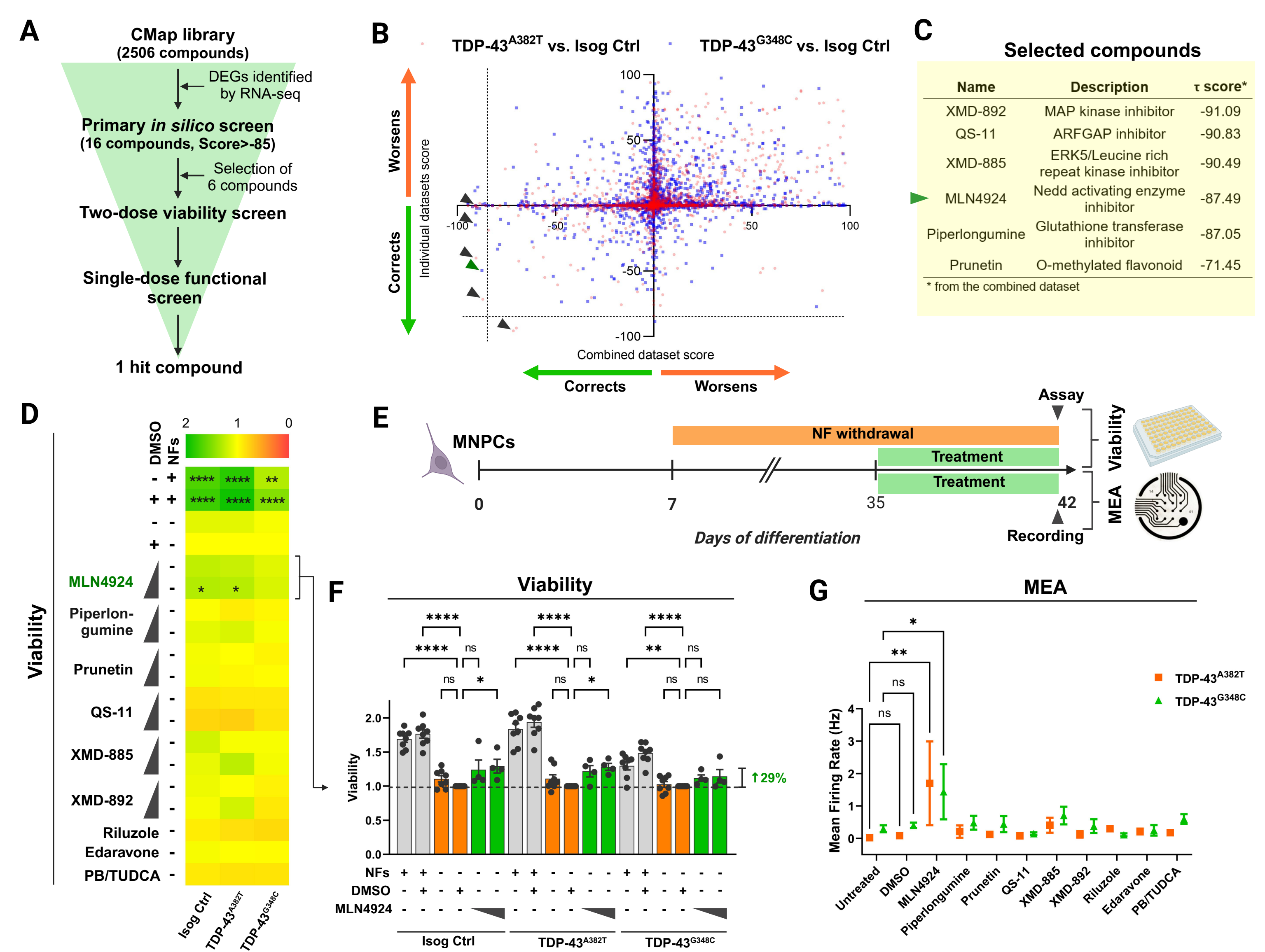


Figure 3. Transcriptome-based *in silico* and phenotypic screens identify one compounds that ameliorates MN survival and activity. (A) Screening funnel used to identify candidate compounds. (B) Scatter plot of the τ scores from the individual (y-axis) versus combined (x-axis) datasets gene signatures. Each data point represent one compound of the CMap library. Arrow heads show selected compounds. (C) Description and τ scores of selected compounds. (D) Heatmap of MN survival relative to DMSO control after treatment with compounds (0.1 μ M and 1.0 μ M) in culture conditions without neurotrophic factors (NFs) supplementation. (E) Overview of phenotypic screens. (F) MN viability after treatment with MLN4924. (G) Mean firing rate of MNs treated with candidates compounds (1.0 μ M). n=4. All data shown as mean \pm SEM. * p <0.05, ** p <0.01, *** p <0.001, **** p <0.0001.

CONCLUSION

We performed whole-transcriptome profiling of MNs differentiated from two knock-in iPSC lines expressing TDP-43^{A382T} or TDP-43^{G348C}. Using mutation-induced gene expression signatures and the CMap database [6], we identified several compounds predicted to normalize gene expression toward wild-type levels. Among top-scoring compounds selected for further investigation, the NEDD8-activating enzyme inhibitor MLN4924 effectively improved viability and neuronal activity, highlighting a possible role for the NEDDylation pathway in the pathobiology of TDP-43-ALS.

ACKNOWLEDGEMENTS

We acknowledge Dr. Rhalena A. Thomas for guidance on sample preparation for RNA-seq. We are also grateful to Dr. Gary A.B. Armstrong and Dr. Vincent Soubannier for creative discussions and their advice. S.L. was supported by the Faculty of Medicine and Health Sciences of McGill University. This work was supported by the Canada First Research Excellence Fund, awarded through the Healthy Brains, Healthy Lives initiative at McGill University; the CQDM FACS program; and the US Department of Defense ALS Research Program. All figures and schematics were created with BioRender.com.



REFERENCES

- Ratti A, Buratti E. J Neurochem. 2016; 1:95-111.
- Delahaye-Duriez A, Srivastava P, Shkura K et al. Genome Biol. 2016; 17:245.
- Readhead B, Hartley BJ, Eastwood BJ et al. Nat Commun. 2018 1; 9:4412.
- Swarup V, Hinz FI, Rexach JE et al. Nat Med. 2019; 25:152-64.
- Lépine S, Nauleau-Javaudin A, Deneault E et al. BioRxiv. 2023.
- Subramanian A, Narayan R, Corsello SM et al. Cell. 2017; 171:1437-1452.